Spectral formulation of turbulent flame speed with consideration of hydrodynamic instability

Swetaprovo Chaudhuri,* V'yacheslav Akkerman, and Chung K. Law
Department of Mechanical and Aerospace Engineering, Princeton University, Princeton, New Jersey 08544-5263, USA
(Received 3 April 2011; published 19 August 2011)

Effects of Darrieus-Landau (DL) instability on the structure and propagation of turbulent premixed flame fronts are considered. By first hypothesizing separation of time scales of instability and turbulence, we estimate whether the instability can develop in the presence of turbulence of given flow rms-velocity and integral length scale. As a result, we modify the standard turbulent premixed combustion regime diagram by introducing new boundaries, limiting the domain where the instability influences the global flame shape and speed. Based on this analysis, a "turbulence-induced DL cutoff" as a function of turbulence and instability parameters is introduced, which when combined with a turbulent flame speed without DL instability yields the turbulent flame speed accounting for the instability. The consumption turbulent flame speed for no DL instability is formulated from the spectral closure of the G equation, thus accounting for the scale-dependent "turbulent" nature of the problem. Finally, an analytical form of the turbulent flame speed is derived, which is found to agree well with the corresponding experimentally measured turbulent flame speed from literature over wide ranges of normalized turbulence intensities and length scales.

DOI: 10.1103/PhysRevE.84.026322 PACS number(s): 47.70.Pq, 47.27.−i, 47.20.−k

I. INTRODUCTION

A turbulent flow is characterized by its turbulence intensity, measured by the turbulent root-mean-square (rms) velocity $U_{\rm rms}$, the integral turbulence length scale λ_I, the kinetic energy budget over various length scales, dissipation, higher moments, etc., while a premixed flame is described by its unstretched laminar propagation speed S_L and the thermal flame thickness δ_L, estimated conventionally as $\delta_L = D_{\rm th}/S_L$, where $D_{\rm th}$ is the thermal diffusivity of the fresh gas. Depending on the scaled values $U_{\rm rms}/S_L$ and λ_I/δ_L, turbulent burning proceeds in several regimes, with different properties and applications for each regime, as shown in the celebrated turbulent combustion regime diagram in Fig. 1 (see, for example, [1–3]).

While the regime diagram provides a useful classification of the possible modes of turbulent combustion, there are processes and factors that are expected to be important in turbulent combustion but have not been integrated into the diagram. One such process is wrinkling of the embedded flamelets due to intrinsic flame-front cellular instabilities, particularly the omnipresent hydrodynamic, Darrieus-Landau (DL) instability caused by the density jump across the flamelets. At issue here is the role of thermal expansion on the structure and dynamics of the flamelets, recognizing that the majority of turbulent flame theories were developed within the Landau limit of an infinitely thin flame front of either zero or small thermal expansion, for near-unity expansion factor $\Theta \equiv \rho_u/\rho_b$, such that the flame does not influence the external turbulent flow and is also hydrodynamically stable [4–8]. In reality, thermal expansion is typically as large as $\Theta = 5-8$, so the flame front modifies the turbulent flow and is also subjected to the hydrodynamic instability [9–12].

Only a few theoretical works have accounted for both turbulence and DL instability [13–17]. In particular, the theory of Bychkov and co-workers [17], based on renormalization [5,8] with scale-invariant flame and turbulence properties, predicts a monotonic increase in the global flame speed with the turbulence intensity, and as such does not describe the possibility that turbulence can also reduce or even suppress DL instability. Indeed, subsequent numerical simulation [18] demonstrated a nonmonotonic dependence of the global flame speed on the turbulence intensification, showing that weakly turbulent flames, with say $U_{\rm rms}/S_L < 0.5$, can actually propagate statistically *slower* than the corresponding corrugated laminar flame.

The present work aims to further examine the effects of turbulence on the development of DL instability and consequently, the turbulent flame structure and propagation speed. Using the hypothesis of separation of DL instability and turbulence time scales, we shall assess whether the instability can develop in the presence of turbulence of given intensity and integral length scale. We shall subsequently modify the regime diagram of Peters [1] by introducing new boundaries that delineate the influence of the instability on the global flame morphology and speed. We shall then propose an expression for the turbulent flame speed based on the concept of a turbulence-induced DL cutoff, superposed on the turbulent flame speed without DL instability. To derive an expression for the turbulent flame speed in the absence of DL instability, a spectral formulation of the G equation proposed by Peters [19] is considered. The turbulent flame speed is then obtained as a functional of the average flame surface dissipation. A simplified analytical result from a physically realizable case is obtained, and is found to agree well with experimental results over a wide range of turbulence intensities and length scales.

The paper consists of three technical sections. The basic formulation and the modified regime diagram are given in Sec. II, while the formulas for a turbulent flame speed are derived in Sec. III.

II. INTERACTION OF DARRIEUS-LANDAU INSTABILITY AND TURBULENCE

We consider a premixed flame propagating in a homogenous isotropic turbulent flow, focusing on the interaction

*Corresponding author: sweto@princeton.edu

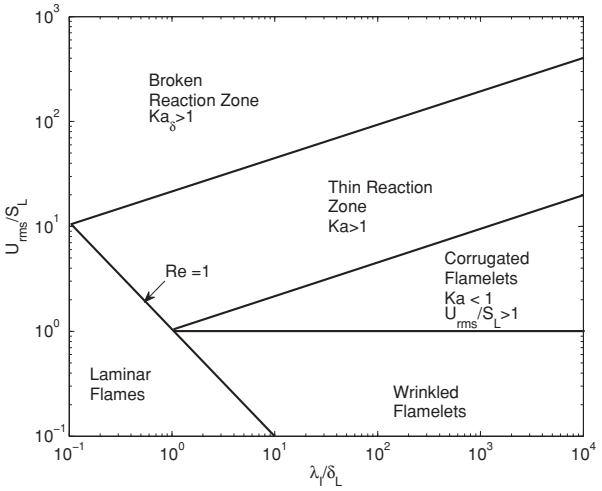

FIG. 1. Turbulent combustion regimes diagram [1].

between turbulence and DL instability over all time and length scales. Consequently, we assume unity Lewis number Le = 1, so as to suppress the diffusional-thermal instability. We further assume that homogeneity and isotropy of turbulence is unaffected by flame propagation such that the constant energy cascade model for homogenous isotropic turbulence as proposed by Kolmogorov can be adopted, recognizing nevertheless that such properties can actually be affected by the embedded flamelets. For example, the inducement of anisotropy through the preferential increase in the normal velocity component in crossing the flame due to thermal expansion is expected.

A. Role of Darrieus-Landau instability

Here we briefly recall the basic ideas behind DL instability, which is caused by thermal expansion in the process of burning, and is inherent to all premixed gaseous flames [10–12].

Within the Landau limit of an infinitely thin flame front, $\delta_L = 0$, the dispersion relation for the growth rate of DL instability takes the form [11]

$$\sigma_{\mathrm{DL}}^{(k)} = \mathrm{X}(\Theta)\, S_L k, \tag{1}$$

where

$$\mathrm{X}(\Theta) = \frac{\Theta}{\Theta+1}[(\Theta+1-\Theta^{-1})^{1/2}-1], \tag{2}$$

with $\mathrm{X} \approx 1.25-1.75$ for typical $\Theta = 5-8$. According to Eq. (1), a flame is absolutely unstable against perturbations of any wave number. Under the first-order approach of small, but finite flame thickness, $\delta_L k \ll 1$, the dispersion relation extends to [20]

$$\sigma_{\mathrm{DL}}^{(k)} = \mathrm{X}(\Theta)\, S_L k\,(1-k/k_c), \tag{3}$$

where the cut-off wave number k_c, related to the DL cut-off wavelength $\lambda_c = 2\pi/k_c$, is given by

$$k_c\delta_L = \left[h_b + \frac{3\Theta-1}{\Theta-1}\mathrm{Mk} - \frac{2\Theta}{\Theta-1}\int_1^\Theta \frac{h(\vartheta)}{\vartheta}d\vartheta + (2\ \mathrm{Pr}-1)\left(h_b - \frac{\int_1^\Theta h(\vartheta)d\vartheta}{\Theta-1}\right)\right]^{-1}. \tag{4}$$

Here the function $h(\vartheta)$ describes the temperature dependence of the transport coefficients, with $h(1) = 1$, $h(\Theta) = h_b$, and Mk is the Markstein number related to the Zel'dovich and Lewis numbers as [21,22]

$$\mathrm{Mk} = \frac{\Theta}{\Theta-1}\int_1^\Theta \frac{h(\vartheta)}{\vartheta}d\vartheta - \frac{\mathrm{Ze}}{2}\frac{\mathrm{Le}-1}{\Theta-1} \times \int_1^\Theta \frac{h(\vartheta)}{\vartheta}\ln\left(\frac{\vartheta-1}{\Theta-1}\right)d\vartheta. \tag{5}$$

Because the present analysis is restricted to the unity Lewis number, Eq. (5) is reduced to

$$\mathrm{Mk} = \frac{\Theta}{\Theta-1}\int_1^\Theta \frac{h(\vartheta)}{\vartheta}d\vartheta. \tag{6}$$

We have $\lambda_c \propto \delta_L$, with $\lambda_c/\delta_L \approx 20-100$ for typical hydrocarbon flames.

According to the Pelce-Clavin dispersion relation (3), all small-scale perturbations with $\lambda < \lambda_c$ are suppressed by thermal conduction, while large-scale perturbations with $\lambda > \lambda_c$ grow exponentially until nonlinear (Huygens) stabilizing effects become important [23]. Consequently, DL instability can be balanced by thermal and nonlinear stabilizations leading to steady propagation of a corrugated, though laminar flame front. Such a flame front has been widely studied analytically [24–26] and computationally [27–29], and the global propagation velocity has been found to be as large as $S_{\mathrm{DL}} \approx (1.5-1.8)S_L$ for $\Theta = 5-8$, which agrees well with the analytical formula [26]

$$\frac{S_{\mathrm{DL}}}{S_L} = 1 + \frac{4\Theta(\Theta-1)^2}{\Theta^3+\Theta^2+3\Theta-1} I\frac{\lambda_c}{\lambda}\left(1 - I\frac{\lambda_c}{\lambda}\right) \approx 1 + \frac{\Theta(\Theta-1)^2}{\Theta^3+\Theta^2+3\Theta-1}, \tag{7}$$

where $I = \mathrm{Int}(\lambda/2\lambda_c + 1/2)$.

If the characteristic length scale of the flame front is very large, exceeding some secondary cut-off value λ_{2c}, then the global steady flame becomes unstable again because the flame front behaves as a set of small "quasiplanar" segments. The size of these segments, however, exceeds λ_c, so they are unstable and become curved [23]. Computational studies [27–29] yield $\lambda_{2c}/\lambda_c \approx 4-4.5$. It has been suggested that DL instability leads to self-similar (say, fractal-like) flame behavior on very large scales, $\lambda \gg \lambda_c$. Then the cut-off wavelength plays the role of the inner cutoff for the fractal cascade, and the propagation velocity of a fractal-like flame front of scale λ can be estimated as

$$S_{\mathrm{DL}}(\lambda) \approx S_L(\lambda/\lambda_c)^D \approx S_{2c}(\lambda/\lambda_{2c})^D, \tag{8}$$

where $S_{2c} = S_{2c}(\lambda_{2c})$ is the propagation velocity of a steady corrugated flame of scale λ_{2c}, Eq. (7), and D is the fractal excess. According to various analytical, computational, and experimental results [29–32], $D \approx 0.25-0.33$ for $\Theta = 5-8$.

The suggested general features regarding Darrieus-Landau instability are therefore (a) DL instability does not develop on small scales, $\lambda < \lambda_c$; (b) it leads to a steady corrugated laminar flame front, Eq. (7), on intermediate scales, $\lambda_c < \lambda < \lambda_{2c}$; and (c) the flame dynamics can assume a self-similar nature,

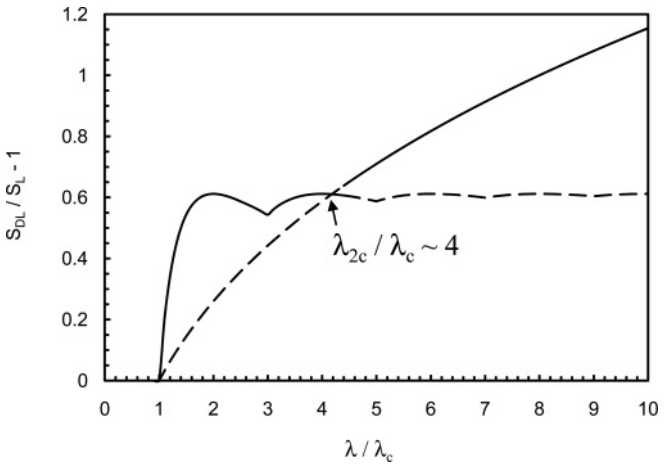

FIG. 2. The global flame velocity resulting from the DL instability versus the length scale of the flow for $\Theta = 7$ and $D = 1/3$.

Eq. (8), on very large scales, $\lambda \gg \lambda_c$, or at least $\lambda > \lambda_{2c}$. These three trends are presented in Fig. 2, where the global flame velocity is plotted versus the length scale of the flow.

B. Separation of instability and turbulence

To investigate the regimes in which the effect of instability is relevant in the presence of turbulence, we first suggest that in strong turbulence, large-scale coherent structures can potentially prevent DL instability to develop and corrugate the flame front. We therefore propose that the instability corrugates the flame in the presence of external turbulence if the characteristic instability growth rate is much greater than the characteristic turbulence eddy frequency. Since our knowledge about nonlinear coupling between various instability modes at realistic thermal expansion is quite limited, within the present formulation the above criterion implies that the characteristic linear, coherent instability growth rate $\sigma_{\mathrm{DL}}^{(k)}$ is much greater than the turbulence eddy frequency $\omega_{\mathrm{turb}}^{(k)}$ that is of the same or smaller wave number, k. Hence, DL instability is sustained in turbulence if

$$\sigma_{\mathrm{DL}}^{(k)} \gg \omega_{\mathrm{turb}}^{(k)}, \tag{9}$$

where $\sigma_{\mathrm{DL}}^{(k)}$ can be estimated by Eq. (3), assuming it is locally valid corresponding to the local laminar flamelet structure.

To justify the above criterion, we consider the flame surface as an initially quasiplanar flamelet, which is simultaneously affected at time $t = 0$ by two single coherent modes related to DL instability and turbulence, both of wave number k. Within the linear approximation, the increase in the flame surface area due to the instability is given by

$$f_{\mathrm{DL}}^{(k)} = A \exp\left(\sigma_{\mathrm{DL}}^{(k)} t\right), \tag{10}$$

while the turbulence eddy can be considered to provide an oscillatory disturbance in the form

$$f_{\mathrm{turb}}^{(k)} = 1 + (k/k_I)^{-m} \sin\left(\omega_{\mathrm{turb}}^{(k)} t\right). \tag{11}$$

Here the amplitude A depends on the initial conditions and can be taken as $A \sim 1$, $k_I = 2\pi/\lambda_I$ is the integral turbulence wave number, and the power factor m can be chosen as $m = 5/6$ considering the Kolmogorov model. Figure 3 presents Eq. (10), as solid, and Eq. (11), as dashed lines. We see that the instability can grow unaffected by the turbulence eddy if $f_{\mathrm{DL}}^{(k)} > f_{\mathrm{turb}}^{(k)}$, which is equivalent to relation (9).

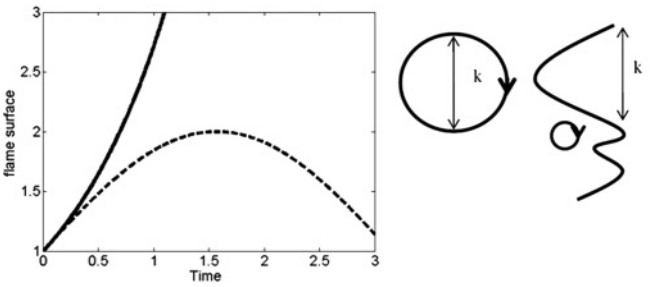

FIG. 3. Exponential instability Eq. (2) (solid), and oscillatory turbulent Eq. (3) (dashed) processes.

It is noted that in order to invoke time-scale separation between these two processes, interaction of the instability and turbulence at the same wave numbers k is considered. This is justified as follows. Wave numbers smaller than k smooth out the effects of the instability, but the corresponding values of $\omega_{\mathrm{turb}}^{(k)}$ are also smaller. Wave numbers larger than k can further corrugate an existing DL-corrugated flamelet at finer scales, since they are related to higher $\omega_{\mathrm{turb}}^{(k)}$, but with amplitudes decreasing as a power law. Hence, statistically, the most relevant wave number of the eddy to interact with the instability such that corrugation by the instability can be suppressed at wave number k is k itself or wave numbers smaller than k, to justify the time-scale separation assumption.

Assuming a constant energy transfer rate, we estimate the eddy turnover time $\tau_{\mathrm{turb}}^{(k)} = 2\pi/\omega_{\mathrm{turb}}^{(k)}$ as

$$\tau_{\mathrm{turb}}^{(k)} = \frac{u_{(k)}^2}{\varepsilon} = \left(\frac{\lambda_I}{U_{\mathrm{rms}}}\right)\left(\frac{k}{k_I}\right)^{-2/3}, \tag{12}$$

where $u_{(k)}^2 \equiv U_{\mathrm{rms}}^2(\lambda/\lambda_I)^{2/3}$ characterizes the kinetic energy of an eddy of size $\lambda = 2\pi/k$, and $\varepsilon \equiv U_{\mathrm{rms}}^3/\lambda_I$ is the mean dissipation rate. This is obtained by the cascade model, where the energy transfer rate across all scales in the inertial subrange is constant and equal to that of the final dissipation [33]. In this work, for simplicity, the integral length scale and that of the largest eddies are assumed to be identical, while in reality they can be related by an $O(1)$ proportionality factor differing from unity. Equations (3), (9), and (12) yield the following criterion for the instability development in the presence of turbulence:

$$\frac{U_{\mathrm{rms}}}{S_L} < \mathrm{X}(\Theta)\left(\frac{k}{k_I}\right)^{1/3}\left(1 - \frac{k}{k_c}\right) \quad \forall k > k_I. \tag{13}$$

This condition can be alternately expressed through a nondimensional parameter

$$\beta = \min_{\forall k > k_I}\left\{\frac{\omega_{\mathrm{turb}}^{(k)}}{\sigma_{\mathrm{DL}}^{(k)}}\right\} = \min_{k_c > k > k_I}\left\{\frac{U_{\mathrm{rms}}}{\mathrm{X}\,S_L}\left(\frac{k_I}{k}\right)^{1/3}\left(1 - \frac{k}{k_c}\right)^{-1}\right\}. \tag{14}$$

Then the criterion above states that the instability develops, with at least one perturbation mode: k, if $\beta < 1$. The parameter

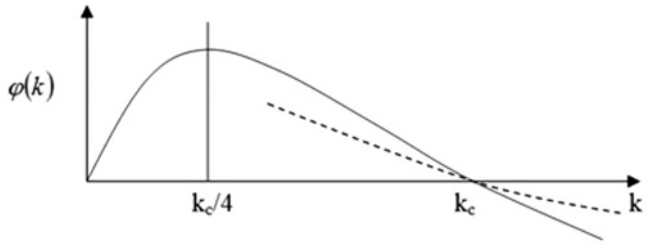

FIG. 4. The function $\varphi(k)$, Eq. (15) versus k in the events of $k_I \leqslant k_c/4 < k_c$ (dashed) and $k_I \leqslant k_c/4$ (solid).

β varies nonmonotonically with k, as demonstrated in Fig. 4 through the function

$$\varphi = (k/k_I)^{1/3}\,(1 - k/k_c)\,, \tag{15}$$

with the dashed and solid lines relating to the domains of $k_c/4 < k_I < k_c$ and $k_I \leqslant k_c/4$, respectively. Within the domain of $k_c/4 < k_I < k_c$, i.e., $\lambda_c < \lambda_I < 4\lambda_c$, Eq. (14) yields

$$\beta = \frac{U_{\rm rms}}{\mathrm{X}\,S_L}\left(1 - \frac{\lambda_c}{\lambda_I}\right)^{-1}, \tag{16}$$

while in the other domain, $k_I \leqslant k_c/4$, i.e., $\lambda_I \geqslant 4\lambda_c$, Eq. (14) predicts a self-similar formula

$$\beta = \frac{4^{4/3}}{3\mathrm{X}}\frac{U_{\rm rms}}{S_L}\left(\frac{\lambda_c}{\lambda_I}\right)^{1/3}. \tag{17}$$

The result (17) resembles the turbulent Karlovitz number $\mathrm{Ka} = (U_{\rm rms}/S_L)^{3/2}(\delta_L/\lambda_I)^{1/2}$. According to Eq. (17), $\beta \propto \mathrm{Ka}^{2/3}$. Clearly, the transition between the trends given by Eqs. (16) and (17) occurs at the scale $4\lambda_c$. With $\beta = 1$ and $\lambda_I = 4\lambda_c$, we find the transitional turbulence intensity

$$U_{\mathrm{rms},T} = \tfrac{3}{4}\mathrm{X}(\Theta)\,S_L, \tag{18}$$

which is about S_L for typical $\Theta = 5{-}8$.

We next observe two interesting effects, common for both turbulent and laminar flames. First, the transitional scale $4\lambda_c$, relevant to turbulent combustion, well fits the secondary cut-off wavelength $\lambda_{2c} \approx (4{-}4.5)\lambda_c$ of the laminar DL instability, discussed in Sec. II A. Second, Eq. (17) states that

$$U_{\rm rms} = (3\mathrm{X}\beta/4^{4/3})S_L(\lambda_I/\lambda_c)^{1/3} \propto (\lambda_I/\lambda_c)^{1/3}. \tag{19}$$

Then, estimating the turbulent flame speed in the form $S_T \propto U_{\rm rms}$ [1,19], which is relevant for high turbulence intensities [8,15,17], we find $S_T \propto (\lambda_I/\lambda_c)^{1/3}$. This agrees with the laminar corrugated flame speed at large scales, Eq. (8). Since the estimate $S_T \propto U_{\rm rms}$ is not necessarily accurate, in Sec. III we discuss an alternate formula for the turbulent flame speed.

We note that a parameter similar to Eq. (17) has also been considered by Bychkov [15] within the renormalization formulation of strongly turbulent combustion, although the related parameter $\tilde{\beta} = (U_{\rm rms}/S_L)(\lambda_I/\lambda_c)^{1/3}$ does not contain the DL-related coefficient $4^{1/3}/3\mathrm{X}(\Theta)$, which is about unity. Consequently, it supports the present formulation, suggesting that at large scales the value $\mathrm{Ka}^{2/3}$ rather than Ka is a key quantity for turbulent combustion. Furthermore, we

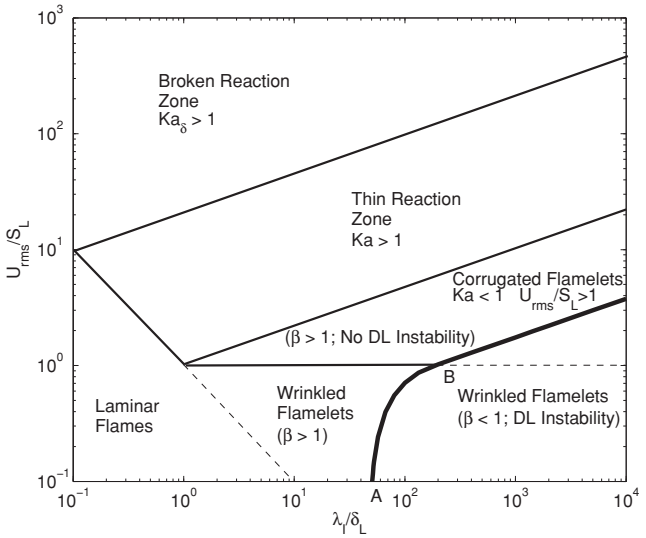

FIG. 5. Modified turbulent combustion regimes diagram.

demonstrate here that the DL parameters such as thermal expansion have to be included in the formulation.

Using the above results, in Fig. 5 we have modified the regime diagram of Fig. 1 by including the bold, solid curve $\beta = 1$, which determines whether DL instability can develop in the presence of turbulence. Thus the instability develops in the domain below this curve for $\beta < 1$. The segment of the curve, AB, with $\lambda_c < \lambda_I < 4\lambda_c$, is given by Eq. (16), indicating that the instability develops at weak turbulence, with $U_{\rm rms} < \mathrm{X}\,S_L(1 - \lambda_c/\lambda_I)$. As for the self-similar domain, Eq. (17), with $\lambda_I \geqslant 4\lambda_c$, here the turbulence intensity should exceed $(3\mathrm{X}S_L/4^{4/3})(\lambda_I/\lambda_c)^{1/3}$ to suppress DL instability.

It is noted that Boughanem and Trouve [14] also introduced an instability domain based on comparing stretch induced by the instability and turbulence. The deduced regime separation curve, however, monotonically increases to high $U_{\rm rms}/S_L$, with decreasing λ_I/δ_L, hence the limiting, well-established case of the DL cutoff for laminar flames, i.e., $U_{\rm rms}/S_L \to 0$, is not captured. In a recent work by Creta *et al.* [34] the Sivashinsky equation was solved in the presence of flow perturbations simulating weak turbulence. It was found that at high turbulence intensity the effect of instability is completely shadowed, thus offering conceptual substantiation of the present approach.

C. Turbulence-induced DL cutoff

It is suggested above that turbulence does not allow DL instability to develop in the domain with $\beta > 1$, i.e., above the line $\beta = 1$ in Fig. 5, while the instability can occur in the domain below it, where $\beta < 1$. Nevertheless, even in the latter case, the effect of DL instability is modified by turbulence as compared to the laminar case. Here we estimate the extent of such moderation in terms of the turbulence scale and intensity.

To arrive at such an estimate, we introduce the concept of a turbulence-induced DL cutoff, $\tilde{\lambda}_c$, determined by the integral turbulence length, λ_I, taken at $\beta = 1$. As a result, we have the turbulence-induced DL cutoff as a function of the laminar DL cutoff and the turbulence intensity, $\tilde{\lambda}_c = \tilde{\lambda}_c(\lambda_c, U_{\rm rms})$, in

the form

$$\frac{\tilde{\lambda}_c}{\lambda_c} = \begin{cases} \left(1 - \frac{3}{4}\frac{U_{\rm rms}}{U_{{\rm rms},T}}\right)^{-1}, & U_{\rm rms} \leqslant U_{{\rm rms},T} \\ 4\left(\frac{U_{\rm rms}}{U_{{\rm rms},T}}\right)^3, & U_{\rm rms} > U_{{\rm rms},T} \end{cases}, \tag{20}$$

with the transitional turbulence intensity $U_{{\rm rms},T}$ given by Eq. (18). Equation (20) states that $\tilde{\lambda}_c = \lambda_c$ in the absence of turbulence, $U_{\rm rms} = 0$, but the turbulence-induced DL cutoff grows with turbulence intensification. This means that increasing turbulence intensity limits the instability development to large scales, thereby moderating the entire effect of the instability.

Because the characteristic time of the instability development is much shorter than that of turbulence, for the present formulation we superpose both effects, considering their contributions to the flame corrugation separately. It is noted that while a theory of the DL evolution of a laminar, initially planar flame segment, discussed in Sec. II A, includes the energy release through Θ and the laminar thermochemical flame properties through λ_c, it does not include parameters of the external flow. We therefore propose that the *partial* contribution from the effects of DL instability on the turbulent flame speed still has the same functional form as that in the laminar case, with λ_c replaced by $\tilde{\lambda}_c$, assuming that all influences of turbulence on the development of DL instability are exhausted by modifying the DL cutoff. For instance, if we know the role of laminar DL instability in the form $S_{\rm DL,lam} = S_L f_{\rm DL}(\lambda_c)$, then we can describe its turbulent counterpart as

$$S_{\rm DL,turb} = S_L f_{\rm DL}(\tilde{\lambda}_c). \tag{21}$$

Here $f_{\rm DL}(\tilde{\lambda}_c) \equiv 1$ if $\lambda_I < \tilde{\lambda}_c$, i.e., the instability is suppressed by turbulence and thermal stabilization. If $\tilde{\lambda}_c < \lambda_I < 4\tilde{\lambda}_c$, then $f_{\rm DL}$ can be estimated by modifying Eq. (7),

$$f_{\rm DL}(\tilde{\lambda}_c) \approx 1 + \frac{4\Theta\,(\Theta-1)^2}{\Theta^3+\Theta^2+3\Theta-1} I \frac{\tilde{\lambda}_c}{\lambda_I}\left(1 - I\frac{\tilde{\lambda}_c}{\lambda_I}\right),$$
$$I = {\rm Int}(\lambda_I/2\tilde{\lambda}_c + 1/2), \tag{22}$$

or even by the approximation in Eq. (7), which does not include scale dependence,

$$\tilde{f}_{\rm DL} \approx 1 + \frac{\Theta\,(\Theta-1)^2}{\Theta^3+\Theta^2+3\Theta-1}. \tag{23}$$

Finally, in the domain of primary interest, $\lambda_I \geqslant 4\tilde{\lambda}_c$, i.e., $\lambda_I \geqslant \tilde{\lambda}_{2c}$, we have

$$f_{\rm DL}(\tilde{\lambda}_c) \approx (\lambda_I/\tilde{\lambda}_c)^D \approx (\lambda_I/\tilde{\lambda}_c)^{1/3},$$
$$S_{\rm DL,turb} \approx S_L(\lambda_I/\tilde{\lambda}_c)^{1/3}. \tag{24}$$

This approach can also be supported by its qualitative similarity to the classical *filtering* formulation, widely adopted in large eddy simulations (LES), which yields the full consideration of large-scale flows, with subgrid modeling on small, subfilter scales. Indeed, the laminar DL cutoff λ_c can be treated as an "effective hydrodynamic flame thickness," since the internal flame structure has to be accounted for $\lambda < \lambda_c$, while the flame sheet approach can be adopted for $\lambda \gg \lambda_c$. Consequently, $\tilde{\lambda}_c$ resembles a "filter size," with "subgrid modeling" according to Eq. (20), and it is reasonable to assume a similar functional dependence for laminar and turbulent DL instability flame speeds.

As a result, we have developed a model which accounts for the moderation of the DL effects due to turbulence, based on the concept of a laminar flamelet with a turbulence-induced DL cutoff. This model has the following features: it reproduces pure laminar effects in the absence of turbulence, $U_{\rm rms} = 0$; it shows the reduction in the DL effects with turbulence intensification; and it shows no effect of DL instability above the boundary $\beta = 1$ in the modified regimes diagram (Fig. 5).

We emphasize that the quantity $S_{\rm DL,turb}$ incorporates only partial contributions from DL instability. It is *not* the global turbulent flame speed S_T, which should also include pure kinematic and dynamical features of flame-flow interaction as derived in Sec. III. A general expression for S_T is expected to have the form

$$S_T = S_{\rm DL,turb} f_T = S_L f_{\rm DL}(\tilde{\lambda}_c) f_T, \tag{25}$$

where f_T is the turbulent flame speed contribution without considering DL instability, which will be discussed in the next section. Regarding the nature of S_T/S_L to be obtained, the concept of a turbulence-induced DL cutoff yields self-similarity in small $U_{\rm rms}/S_L$ if $\lambda_I \geqslant 4\tilde{\lambda}_c$ and a statistically steady front when $\tilde{\lambda}_c < \lambda_I < 4\tilde{\lambda}_c$, i.e., in moderate $U_{\rm rms}/S_L$. However, the range of $\tilde{\lambda}_c < \lambda_I < 4\tilde{\lambda}_c$ is the domain where β is only slightly less than unity, and hence an uncertain zone in the modified regime diagram in Fig. 5 regarding its form and existence in the context of the current study. As such, in this paper we extrapolate the concept of self-similarity in the entire regime of $\lambda_I \geqslant \tilde{\lambda}_c$. This is justified as self-similarity and is observed in the secondary instability, i.e., in DL-corrugated flames. In the turbulent case, at moderate $U_{\rm rms}/S_L$ the flame surface is already corrugated by turbulence. Hence it is reasonable to expect that DL instability, if prevailing in this region, is governed by self-similarity.

III. TURBULENT FLAME SPEED

The propagation of either laminar or turbulent premixed flames in complex flow geometries has often been analyzed using the G equation [10]. For the turbulent flame speed, the G equation along with the flame surface density equation or the progress variable approach, namely, the Bray-Moss-Libby model, have been used in the framework of Reynolds-averaged Navier-Stokes (RANS) equation formulations [35–38]. However, a RANS model with $k-\varepsilon$ type closures cannot consider the scale-dependent evolution of global properties; in general, the multiscale nature of turbulence in premixed combustion has been considered only in very few analytical studies. In particular, Peters [19] proposed a spectral closure of the G equation on the basis of dimensional arguments and extended that in [39] to include effects of the velocity field induced by gas expansion. A more rigorous but complicated approach was adopted by Collins and co-workers [40,41] by using the Eddy Damped Quasi Normal Markovian (EDQNM) approximation, which is one of the statistical closure theories for nonreacting turbulence. All these approaches utilize the turbulent flame surface spectra with dissipation arising from flame properties such as the flame speed and the Markstein length, $\delta_M = \delta_L\,{\rm Mk}$, with the Markstein number Mk given within the approach of unity Lewis number by Eq. (6). In nonreacting turbulent flows in pipes, it has been recently shown that the energy spectrum

can predict global properties such as the friction factor [42]. Hence, by this recent example and many others, it is recognized that a physics-based derivation of any global property in a turbulent flow, including the turbulent flame speed, needs to consider the scale dependency of the problem.

A. Spectral closure of G equation

To analyze the turbulent flame speed without considering DL instability, we use the spectral closure of the G equation proposed by Peters [19]. Although the closure is based on simple dimensional arguments, it has been shown by Direct Numerical Simulation (DNS) [43] and experiments [44] that the scalar spectrum function agrees well with the spectrum derived by spectral closure of the G equation [19]. The G equation takes the form

$$\frac{\partial G}{\partial t} + \mathbf{V}\cdot\nabla G = [S_L - S_L\delta_M\kappa + \delta_M \mathbf{n}\cdot\nabla\mathbf{v}\cdot\mathbf{n}]\,|\nabla G|\,, \quad (26)$$

with G describing the flame surface accounting for stretch effects, κ being the local curvature, and $\mathbf{n}$ being the flame surface normal.

A statistically planar premixed flame front, propagating in mean in the z direction in a homogeneous isotropic turbulent flow, can be described as $G(x,y,z,t) = z(t) + g(x,y,z,t)$ such that large gradients due to mean propagation in the z direction are removed from g. The scalar autocorrelation function for g is given by $R(\mathbf{r},t) \equiv \langle g(\mathbf{x},t)g(\mathbf{x}+\mathbf{r},t)\rangle$. The statistical quantity R is assumed to be isotropic, and hence is a function of $\mathbf{r}$ only. Then the transport equation of the autocorrelation function $R(\mathbf{r},t)$ can be obtained from Eq. (26) by invoking conditions of local homogeneity as

$$\frac{\partial R}{\partial t} + 2\frac{\partial \langle u_i(\mathbf{x}+\mathbf{r},t)g(\mathbf{x},t)g(\mathbf{x}+\mathbf{r},t)\rangle}{\partial r_i} + 2S_L S_1 + 2D_L S_2 + 2\delta_M S_3 = 0, \quad (27)$$

where

$$S_1(r,t) = -\langle g(\mathbf{x}+\mathbf{r},t)\sigma'(\mathbf{x},t)\rangle, \quad \sigma = |\nabla G|\,,$$

$$S_2(r,t) = -\left\langle g(\mathbf{x}+\mathbf{r},t)\left(\frac{\partial^2 G(\mathbf{x},t)}{\partial x_i^2} - \frac{\partial \ln\sigma(\mathbf{x},t)}{\partial x_j}\frac{\partial G(\mathbf{x},t)}{\partial x_j}\right)'\right\rangle,$$

$$S_3(r,t) = -\left\langle g(\mathbf{x}+\mathbf{r},t)\left(\frac{\partial v_i(\mathbf{x},t)}{\partial x_j}\frac{\sigma_i(\mathbf{x},t)\sigma_j(\mathbf{x},t)}{\sigma(\mathbf{x},t)}\right)'\right\rangle. \quad (28)$$

The second term in Eq. (27) is due to convective transport, while the quantities S_1, S_2, and S_3 given by Eq. (28) describe kinematic restoration, scalar dissipation, and strain-scalar covariance, respectively [19]. It was shown by DNS calculations [39] that the last term (S_3) in Eq. (28) is of minor importance in the corrugated flamelets regime.

The quantity R can be written as a Fourier series

$$R(\mathbf{r},t) = \sum_{\mathbf{k}} \hat{R}(\mathbf{k},t)\exp(i\mathbf{k}\cdot\mathbf{r})\,. \quad (29)$$

Then the scalar spectrum function is defined as [33]

$$\Phi(\bar{\mathbf{k}},t) = \sum_{\mathbf{k}} \delta(\bar{\mathbf{k}}-\mathbf{k})\hat{R}(\mathbf{k},t), \quad (30)$$

where $\bar{\mathbf{k}}$ is a continuous wave-number variable and δ is the Dirac delta function. Integrating Eq. (30) over a sphere in Fourier space, with a surface boundary $S(k)$, we remove the directional dependence of $\mathbf{k}$, arriving at the *scalar spectrum function* $\Gamma(k,t)$ in the form

$$\Gamma(k,t) = \oint \Phi(\mathbf{k},t)dS(k) = 4\pi k^2\hat{R}(k,t). \quad (31)$$

Following the same procedure for all other terms in Eq. (27), we obtain the transport equation for $\Gamma(k,t)$,

$$\frac{\partial\Gamma(k,t)}{\partial t} - T(k,t) + 4\pi k^2[2S_L\hat{S}_1(k,t) + 2D_L\hat{S}_2(k,t)] = 0, \quad (32)$$

where $T(k,t)$ stands for the integrated-within-$S(k)$ Fourier transform for the collective transport terms in Eq. (28), while $\hat{S}_1(k,t)$ and $\hat{S}_2(k,t)$ are the integrated-within-$S(k)$ Fourier transforms for the kinematic restoration and scalar dissipation, respectively. The transport terms of the Fourier transforms of the transport equation for Γ were closed by Peters [19], similar to those closed by Pao [45] for a passive scalar in homogenous isotropic turbulence, by the gradient transport assumption and dimensional consistency such that

$$T(k,t) = -\frac{\partial W(k,t)}{\partial k}, \quad W(k,t) = C_s^{-1}\varepsilon^{1/3}k^{5/3}\Gamma(k,t). \quad (33)$$

The coefficient C_s^{-1} is a universal constant of the scalar spectrum similar to the Kolmogorov constant in the energy spectrum. The last terms in Eq. (32) are closed on the basis of dimensional consistency as

$$8\pi k^2\hat{S}_1 = c_1 C_s^{-1}k\Gamma, \quad 8\pi k^2\hat{S}_2 = c_2 C_s^{-1}k^2\Gamma, \quad (34)$$

with the modeling constants c_1 and c_2. Then Eq. (32) can be analytically integrated as

$$\Gamma(k) = BHk^{-5/3}\exp\{-3c_1(L_G k)^{1/3}\}\exp\left\{-\tfrac{3}{4}c_2(L_C k)^{4/3}\right\}, \quad (35)$$

where B is the integration constant and $H = H(k-k_I)$ is a function determined from initial conditions. Here H is chosen to be a Heaviside step function, i.e., $H = 0$ if $k < k_I$ and $H = 1$ otherwise, in such a manner that Γ is independent of time. Substituting the Gibson scale $L_G = (S_L/U_{\rm rms})^3\lambda_I$ and the Corrsin scale $L_C = (D_L^3/\varepsilon)^{1/4}$ into Eq. (35), we finally obtain

$$\Gamma(k) = BH(k-k_I)k^{-5/3}\exp\left[-3c_1(2\pi)^{1/3}\left(\frac{U_{\rm rms}}{S_L}\right)^{-1}\left(\frac{k}{k_I}\right)^{1/3}\right] \times \exp\left[-\frac{3}{4}(2\pi)^{4/3}c_2\left(\frac{U_{\rm rms}}{S_L}\right)^{-1}\left(\frac{k_I}{k_M}\right)\left(\frac{k}{k_I}\right)^{4/3}\right], \quad (36)$$

with the "Markstein" wave number $k_M = 2\pi/\delta_M = 2\pi/\delta_L$ Mk. Thus in the final form of the scalar spectrum, the universal $-5/3$ power k dependence is retained, arising from the kinetic energy transfer between the flow and the flame, and resulting in folds of different length scales, in addition to two exponentially decaying dissipation terms resulting from the kinematic restoration and finite curvature limitation due to finite flame thickness.

B. Approximation of the turbulent flame speed

By definition from [6], the turbulent flame speed of a corrugated flame front, scaled by the unstretched laminar flame speed, is given by

$$S_{T,0}/S_L = \langle|\nabla G|\rangle = \langle\sqrt{(\nabla\langle G\rangle + \nabla g)\cdot(\nabla\langle G\rangle + \nabla g)}\rangle = \langle\sqrt{1+\nabla g\cdot\nabla g + 2(\partial g/\partial z)}\rangle \quad (37)$$

as $\langle G\rangle = z$, so $\nabla\langle G\rangle = \hat{k}$. It is recognized that this definition is not limited by flame folding, and hence g can be a multiple-valued function [6]. Moreover, according to [39], the G equation formulation adopted here is valid in both the corrugated flamelets regime as well as the thin reaction zone regime. For mathematical tractability, local effects of the laminar flame speed are neglected but could be included in future studies when exact joint correlations of curvature and strain with $|\nabla G|$ are known. It can be argued that constant laminar flame speed is a valid assumption when Le = 1 as $S_{T,0}/S_L$ should be mostly independent of strain and curvature since both are nearly symmetric, zero-centered distributions in strong turbulence [46]. To summarize, although the effect of strain and curvature may not affect the global burning rate through variation of local flame speed for Le = 1, they do affect the total flame surface area, and hence should be considered in the governing equation of the surface evolution as in Eq. (27).

The term $\partial g/\partial z$ is identically zero when g is single valued in $\{x,y\}$, i.e., $g = g(x,y,t)$. Clearly comparing the orders of the gradient-squared and z-derivative terms, the latter is important only when $S_{T,0}/S_L \sim$ 1–2, which is expected at very weak turbulence. But then the flame surface is expected to be single valued in $\{x,y\}$, and hence the last term is identically zero. Furthermore, it has been shown from DNS [41] that the z-derivative term can be neglected without loss of generality as its contribution to the turbulent flame speed, arising from multiple crossing of the flame surface in the z direction, is negligible. Consequently, Eq. (37) reduces to

$$S_{T,0}/S_L = \langle\sqrt{1+\nabla g\cdot\nabla g}\rangle. \quad (38)$$

The quantity g can be considered as a random function such that $\langle g\rangle = 0$ and $\langle\partial g/\partial x_i\rangle = 0$. Determining the turbulent flame speed then poses a mathematical difficulty, since $S_{T,0}/S_L$ is averaged over the square root containing the square of ∇g. For $\nabla g\cdot\nabla g \ll 1$, the quantity $S_{T,0}/S_L$ can be approximated as

$$S_{T,0}/S_L = \langle\sqrt{1+\nabla g\cdot\nabla g}\rangle \approx \left\langle 1+\tfrac{1}{2}\nabla g\cdot\nabla g\right\rangle = 1+\tfrac{1}{2}\langle\nabla g\cdot\nabla g\rangle, \quad (39)$$

which has been widely adopted. This approach is restricted to only very weakly corrugated fronts, say, with $S_{T,0}/S_L < 2$. There exists no simple approximation for $S_{T,0}/S_L$ in the opposite limit of $\nabla g\cdot\nabla g \gg 1$. However, considering g as a one-dimensional random function, with the derivative obeying the Gaussian distribution, Corrsin and Phillips [47] obtained an analytical expression for the contour length of a curve $L = \langle\sqrt{1+(dg/dx)^2}\rangle$, with the standard deviation $\sigma_1 = \sqrt{\langle(dg/dx)^2\rangle}$ in the form

$$L = \frac{\exp\left(1/4\sigma_1^2\right)}{2\sqrt{2\pi}\sigma_1}\left\{K_0\left(\frac{1}{4\sigma_1^2}\right) + K_1\left(\frac{1}{4\sigma_1^2}\right)\right\}, \quad (40)$$

where K_v is the modified Bessel function of the second kind. Figure 6 compares contour length of a function with Gaussian gradient and that of a sine function with same variance. The nature of the functions immediately provides insights into a simple, generalized approximation for such sine and Gaussian processes that hold without the restriction of $\nabla g\cdot\nabla g \ll 1$. As a result, we approximate $S_{T,0}/S_L$ by

$$S_{T,0}/S_L = \langle\sqrt{1+\nabla g\cdot\nabla g}\rangle \approx \sqrt{\langle 1+\nabla g\cdot\nabla g\rangle}. \quad (41)$$

It is evident that approximation (41) holds without any assumption for $\nabla g\cdot\nabla g \ll 1$. Indeed,

$$S_{T,0}/S_L = \langle\sqrt{1+\nabla g\cdot\nabla g}\rangle \approx \left\langle 1+\tfrac{1}{2}\nabla g\cdot\nabla g\right\rangle = 1+\tfrac{1}{2}\langle\nabla g\cdot\nabla g\rangle \approx \sqrt{\langle 1+\nabla g\cdot\nabla g\rangle}. \quad (42)$$

But even without any restriction on the magnitude of the approximation error for sine and Gaussian processes, it is always less than 25% for the one-dimensional case, as evident from Fig. 6.

For a more general two-dimensional case, with g obeying a Gaussian distribution, a contour length obviously becomes an area $\sim S_{T,0}/S_L$, and we have verified numerically in the present study that the approximation error monotonically grows with increasing σ, before saturating to a constant error of about 15%. Experimental and DNS evidence from [48,49] suggests that the quantity $\partial g/\partial x_i$ follows a nearly Gaussian distribution. There is also experimental evidence suggesting that the lower moment, i.e., g, as well as the higher moment, i.e., curvature, follow the Gaussian distribution in strong turbulence as shown in [1] and [48], respectively. On the other hand, it can be argued that turbulent velocity derivative probability density functions (PDFs) are inherently non-Gaussian, and their distributions display exponential tails. Such non-Gaussianity forms the

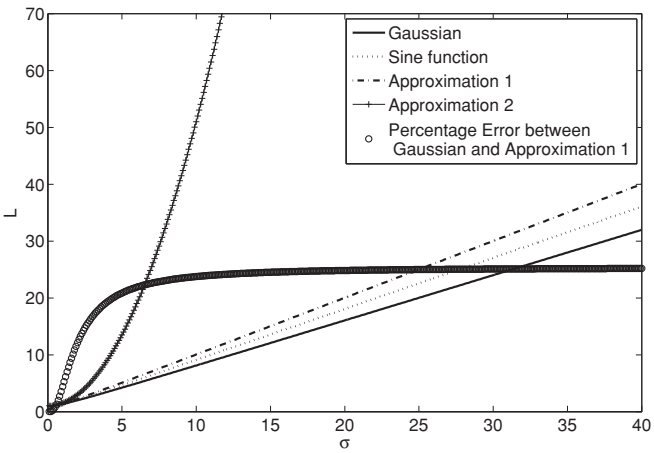

FIG. 6. Contour length i.e., the functional $\langle\sqrt{1+\nabla g\cdot\nabla g}\rangle$ vs. standard deviation when (i) the gradient of g is Gaussian, (ii) g is a sine function, (iii) Approximation 1 given by $\sqrt{\langle 1+\nabla g\cdot\nabla g\rangle}$, (iv) Approximation 2 given by $1+\frac{1}{2}\langle\nabla g\cdot\nabla g\rangle$, and (v) Percentage error involved between (i) and (iii) with regard to (i).

very basis for nonlinear energy transfer, and in nonreacting fluid turbulence the passive scalar gradient squared quantities are typically distributed as log normal instead of Gaussian [50]. Moreover, for a material surface in nonreacting fluid turbulence, $\nabla g \cdot \nabla g$ shows a log-normal distribution, and hence the exact distribution of the quantity is debatable as to whether it is Gaussian or log normal. It is shown below that the approximation of Eq. (41) holds even for the log-normal distribution with standard deviations that are possible in practical flow situations.

Let us consider the approximation for the turbulent flame speed with $\nabla g \cdot \nabla g$ following a log-normal distribution. Substituting $Z = \nabla g \cdot \nabla g$ into Eq. (38), we find the ratio $S_{T,0}/S_L$ to be given by the expectation $E[\Omega]$, where $\Omega = \sqrt{1+Z}$, and Z follows a log-normal distribution with its natural logarithm having the mean μ and the standard deviation σ. Consequently,

$$\frac{S_{T,0}}{S_L} = E[\Omega] = \frac{1}{\sqrt{2\pi\sigma^2}} \int_0^\infty \sqrt{1+Z}\,\frac{1}{Z} \exp\left\{-\frac{(\ln Z-\mu)^2}{2\sigma^2}\right\} dZ. \tag{43}$$

The integral in Eq. (43) can be decomposed as

$$\begin{aligned} E[\Omega] &= \frac{1}{\sqrt{2\pi\sigma^2}} \left[\int_0^1 \sqrt{1+Z}\,\frac{1}{Z} \exp\left\{-\frac{(\ln Z-\mu)^2}{2\sigma^2}\right\} dZ \right. \\ &\quad \left. + \int_1^\infty \sqrt{1+Z}\,\frac{1}{Z} \exp\left\{-\frac{(\ln Z-\mu)^2}{2\sigma^2}\right\} dZ \right] \\ &\approx \frac{1}{\sqrt{2\pi\sigma^2}} \left[\int_0^1 \left(1+\frac{Z}{2}\right)\frac{1}{Z} \exp\left\{-\frac{(\ln Z-\mu)^2}{2\sigma^2}\right\} dZ \right. \\ &\quad \left. + \int_1^\infty Z^{1/2}\,\frac{1}{Z} \exp\left\{-\frac{(\ln Z-\mu)^2}{2\sigma^2}\right\} dZ \right]. \end{aligned} \tag{44}$$

Substituting $Y = \ln Z$ and following the Mellin transform of the log-normal PDF [51], which gives $E[Z^s] = \exp(s\mu + s^2\sigma^2/2)$, and the related integrals from 0 to 1 and from 1 to ∞, we obtain

$$\begin{aligned} E[\Omega] &= \frac{1}{2}\mathrm{erfc}\left(\frac{\mu}{\sigma\sqrt{2}}\right) + \frac{1}{4}\exp\left(\mu+\frac{\sigma^2}{2}\right)\mathrm{erfc}\left(\frac{\sigma^2+\mu}{\sigma\sqrt{2}}\right) \\ &\quad + \frac{1}{2}\exp\left(\frac{\mu}{2}+\frac{\sigma^2}{8}\right)\mathrm{erfc}\left(-\frac{\sigma^2+2\mu}{\sigma 2\sqrt{2}}\right). \end{aligned} \tag{45}$$

As shown in Fig. 7, this expression is well approximated by

$$\begin{aligned} E[\Omega] &\approx \sqrt{1+\exp(-\sigma^2/4)\exp(\mu+\sigma^2/2)} \\ &= \sqrt{1+\exp(-\sigma^2/4)E[Z]}. \end{aligned} \tag{46}$$

In the same figure, the expectations, $E[\Omega] = \langle\sqrt{1+Z}\rangle$, for numerically generated random variable Z, with log-normal distributions over a range of mean and standard deviations, are compared to the analytical expression and the proposed approximation, with good agreement demonstrated. This has been validated by the numerical integration of Eq. (43) as well. Now, for a log-normal distribution the variance is given by

$$\sigma^2 = \ln\{1+\mathrm{var}[Z]/E[Z]^2\} \approx \ln[K], \tag{47}$$

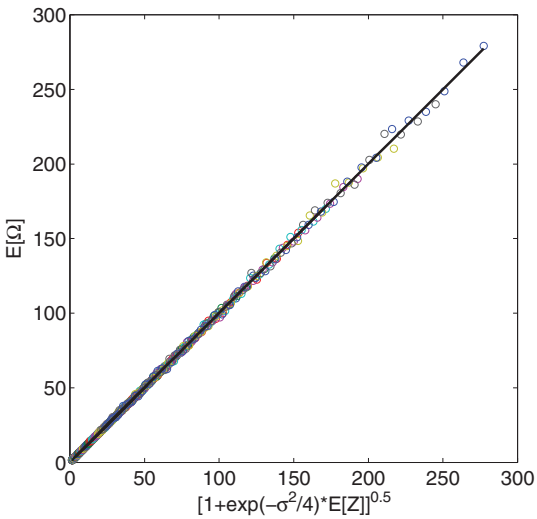

FIG. 7. (Color online) Plot of the exact expectation versus approximation. Symbols: Numerically generated log-normal distribution and black line: analytical expression for $0.1 < \mu < 5$ and $\sigma_1 < \sigma < 5$. Both μ and σ are independently varied.

where K is the flatness of the distribution of $\partial g/\partial x_i$, considering the contribution by the cross terms $\langle(\partial g/\partial x_i)^2(\partial g/\partial x_j)^2\rangle$ to be the same as that of $\langle(\partial g/\partial x_i)^4\rangle$. For either fluid turbulence or a passive scalar in turbulent flow field, it is known that K increases with R_λ in contrary to Kolmogorov's self-similarity hypothesis [50] and is attributed to intermittency. Intermittency of a premixed flame surface is not a well-known topic, but even if we assume the flatness K to be that as found for a passive scalar in nonreacting turbulence, for very high $R_\lambda \sim 10^3$ (where R_λ is the Taylor-scale Reynolds number), which are around an order of magnitude beyond any experimental measurements for the turbulent flame speed so far, we have $K \sim 30$ [52]. Hence $\exp(-\sigma^2/4) = 0.43$ and for all practical purposes $0.43 \ll \exp(-\sigma^2/4) < 1$. Furthermore, since $\exp(-\sigma^2/4)$ is within the square root, the effective correction is $\sim\exp(-\sigma^2/8)$. Thus the maximum error introduced is 35%, which allows this term to be neglected for the sake of simplicity. It can, however, be retained for larger R_λ and can be estimated alternatively as shown below, but in that case the intermittency effects on the flame itself need to be explored further. In all of the formulations in this paper, this exponential term is not retained and is assumed unity unless otherwise stated.

An alternative estimation of σ^2 can be obtained following Kolmogorov's refined similarity hypothesis of 1961 [53], where the log-normal distribution of dissipation was considered. Following [53], the standard deviation of the logarithm of the scalar dissipation rate was proposed as $\sigma^2_{\ln(\chi)_r} \approx \mu_\theta \ln(L_0/r)$, where L_0 and r are the larger ($\sim$integral length scale) and the smaller scales, respectively, while μ_θ is a universal constant according to [53]. Gibson [54] found that μ_θ is indeed a universal constant, $\sim$0.44 in oceanic and galactic scales, where R_λ is so large that turbulence is truly "universal." As has been shown above, for all practical reacting flows encountered, $\exp(-\sigma^2/4) \sim 1$ is probably a good choice as then it avoids the complications with intermittency. But for very large R_λ, where the correction is nontrivial, intermittency

can be considered in a similar manner to that as in [53,54] on the passive scalar g field by proposing

$$\left(\sigma^2_{\ln(\nabla g\cdot\nabla g)}\right)_{\max} \approx \mu_g \ln(\lambda_I/\delta_L) \Rightarrow \exp(-\sigma^2/8) = (\lambda_I/\delta_L)^{-\mu_g/8} \sim (\lambda_I/\delta_L)^{-0.055}. \quad (48)$$

No estimate on μ_g is known so far, and hence the universal constant found in [54] is substituted in Eq. (48). The introduction of intermittency and hence, departure from Kolmogorov's self-similarity hypothesis, is apparent as the nonlinear averaging of $Z = \nabla g \cdot \nabla g$ introduces higher moments.

In summary, by this approximation we have essentially circumvented a closure problem of averaging a nonlinear functional by neglecting higher moments. Gaussian distribution yields constant flatness and hence a constant error. For the log-normal distribution, omission of higher moments could be allowed for weak to moderate intermittency levels of the flame surface dissipation, but for strong intermittency that might be encountered in extreme Reynolds numbers, a correction is proposed in Eq. (48). As such, the approximation is justified in the framework of the two possible distributions considered.

C. Turbulent flame speed through spectral closure

The Fourier transform of the scalar autocorrelation function $R(\mathbf{r},t) \equiv \langle g(\mathbf{x},t)g(\mathbf{x}+\mathbf{r},t)\rangle$ is given by [33]

$$\hat{R}(\mathbf{k},t) = \hat{F}_{\mathbf{k}}\{R(\mathbf{r})\}\,\delta_{\mathbf{k}(-\mathbf{k})} = \langle \hat{g}(\mathbf{k},t)\hat{g}(\mathbf{k}',t)\rangle \delta_{\mathbf{k}(-\mathbf{k}')} = \langle g(\mathbf{k},t)\hat{g}(-\mathbf{k},t)\rangle = \hat{F}_{\mathbf{k}}\{R(\mathbf{r})\}, \quad (49)$$

where

$$\delta_{\mathbf{k}(-\mathbf{k}')} = \begin{cases} 1 & \text{if} \quad \mathbf{k} = \mathbf{k}' \\ 0 & \text{if} \quad \mathbf{k} \neq \mathbf{k}' \end{cases} \quad (50)$$

is the Kronecker delta function and the operator $\hat{F}_{\mathbf{k}}$ determines the coefficient of the Fourier mode of the wave vector $\mathbf{k}$. Consequently,

$$R(\mathbf{r},t) = \sum_{\mathbf{k}} \hat{R}(\mathbf{k},t)\exp(i\,\mathbf{k}\cdot\mathbf{r}) = \int_{-\infty}^{+\infty}\int\int \Phi(\bar{\mathbf{k}})\exp(i\,\bar{\mathbf{k}}\cdot\mathbf{r})\,d\bar{\mathbf{k}}, \quad (51)$$

where $\bar{\mathbf{k}}$ is the continuous wave-number variable and $\Phi(\bar{\mathbf{k}}) = \sum_{\mathbf{k}} \hat{R}(\mathbf{k},t)\delta(\bar{\mathbf{k}}-\mathbf{k})$ is the spectrum function tensor. Hence, $R(\mathbf{0},t) = \int_{-\infty}^{+\infty}\int\int \Phi(\bar{\mathbf{k}})d\bar{\mathbf{k}}$. The Fourier transform of $\mathbf{g}_1 = \nabla g$ is

$$\hat{\mathbf{g}}_1(\mathbf{k}) = \hat{F}_{\mathbf{k}}\left\{\frac{\partial g}{\partial x_j}\mathbf{j}\right\} = \left\langle \mathbf{j}\frac{\partial g}{\partial x_j}\exp(i\mathbf{k}\cdot\mathbf{x})\right\rangle = i\,k_j\hat{g}(\mathbf{k})\mathbf{j}. \quad (52)$$

Now we shall apply the above method to the quantity $\mathbf{g}_1(\mathbf{x},t)$. In particular, we introduce the autocorrelation function of $\mathbf{g}_1$ in the form $R_1(\mathbf{r},t) = \langle \mathbf{g}_1(\mathbf{x},t)\mathbf{g}_1(\mathbf{x}+\mathbf{r},t)\rangle$, with $R_1(\mathbf{0},t) = \langle \mathbf{g}_1(\mathbf{x},t)\mathbf{g}_1(\mathbf{x},t)\rangle$. Similar to Eq. (49) and accounting for Eq. (52), we write

$$\hat{R}_1(\mathbf{k},t) = \langle \hat{\mathbf{g}}_1(\mathbf{k},t)\,\hat{\mathbf{g}}_1(-\mathbf{k},t)\rangle = \langle\{ik_j\hat{g}(\mathbf{k},t)\mathbf{j}\}\{-ik_j\hat{g}(-\mathbf{k},t)\mathbf{j}\}\rangle = \langle k_jk_j\hat{g}(\mathbf{k},t)\,\hat{g}(-\mathbf{k},t)\rangle = k_jk_j\hat{R}(\mathbf{k},t), \quad (53)$$

with $R_1(\mathbf{0},t) = \int_{-\infty}^{+\infty}\int\int \Phi_1(\bar{\mathbf{k}})d\bar{\mathbf{k}}$, where

$$\Phi_1(\mathbf{k}) = \sum_{\mathbf{k}} \hat{R}_1(\mathbf{k},t)\delta(\bar{\mathbf{k}}-\mathbf{k}) = \sum_{\mathbf{k}} k_jk_j\hat{R}(\mathbf{k},t)\delta(\bar{\mathbf{k}}-\mathbf{k}) = \bar{k}_j\bar{k}_j\Phi(\mathbf{k}). \quad (54)$$

Equations (53) and (54) state

$$R_1(\mathbf{0},t) = \langle \nabla g\cdot\nabla g\rangle = \int_{-\infty}^{\infty}\int\int k_jk_j\Phi(\mathbf{k})\,d\mathbf{k} = \int_0^{\infty} k^2\Gamma(k,t)\,dk = \int_0^{\infty} k^2\Gamma(k)\,dk, \quad (55)$$

as Γ is independent of time, which leads to

$$S_{T,0}/S_L = \langle\sqrt{1+\nabla g\cdot\nabla g}\rangle \approx \sqrt{\langle 1+\nabla g\cdot\nabla g\rangle} = \sqrt{1+\int_0^{\infty} k^2\Gamma(k)\,dk} = \sqrt{1+\int_{k_I}^{\infty} k^2\Gamma(k)\,dk}. \quad (56)$$

For numerical calculations the integral was evaluated up to $10k_F$, where $k_F = 2\pi/\delta_L$ is the wave number corresponding to the flame thickness. The quantity Γ in Eq. (56) is given by Eq. (36), with the phenomenological constants B, c_1, and c_2, which can be determined from experiments or direct numerical simulations. For the present study, the value B is chosen in such a manner that the turbulent flame brush thickness is equal to the integral length scale, i.e.,

$$\delta_T \equiv \langle g^2\rangle^{1/2} = \left(\int_{k_I}^{\infty}\Gamma(k)dk\right)^{1/2} = \lambda_I \quad (57)$$

at the maximum $U_{\rm rms}$ in the corrugated flamelets regime for given λ_I and δ_L. It was shown by DNS calculations [55] that the condition $1 < \delta_T/\lambda_I < 1.5$ holds over the range of normalized turbulence intensity, $0.5 < U_{\rm rms}/S_L < 17$. The coefficients c_1 and c_2 are chosen as 0.2 and 2, respectively, under the assumption that dissipation due to flame thickness provides an order of magnitude greater effect than that due to kinematic restoration. Such an assumption is justified, for instance, by DNS of a premixed hydrogen flame in homogenous isotropic turbulence with reduced chemistry [56]. It was found that while determining the turbulent flame surface as a fractal structure, the lower cutoff for departure from self-similarity depends on the flame thickness or the Markstein length and not on the Gibson scale, which is only possible if the first exponential term in Eq. (35) is weak. The reason could be that the gas expansion velocity nearly cancels out the effects of kinematic restoration having the same dimensional dependence, $k\Gamma$ in Eq. (32), as shown by DNS calculations [39], and therefore the effective dissipation is provided by the flame thickness alone. Thus the dissipation effect due to flame thickness is expected to dominate over that due to effective kinematic restoration given by the Gibson scale because of the strong gas expansion effects. Thus the thermal expansion effects implicitly enter into the no DL instability formulation for $S_{T,0}/S_L$ as well.

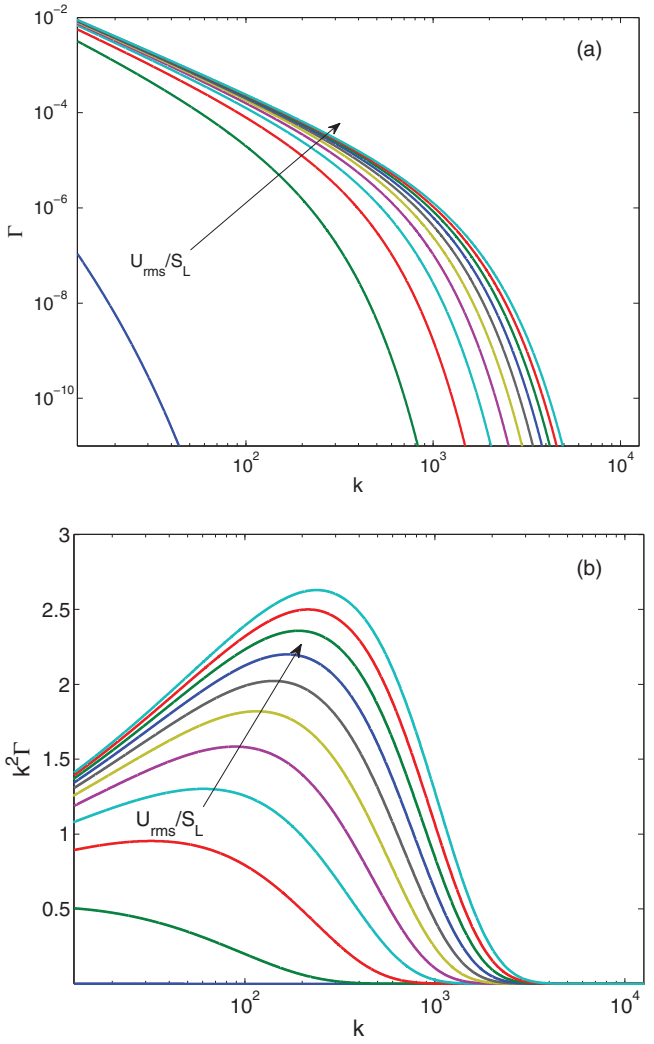

FIG. 8. (Color online) Spectra of Γ (a) and $k^2\Gamma$ (b) versus k with fixed $\lambda_I/\delta_L = 10^3$ and at $U_{\rm rms}/S_L = 0.1$, and 1–10 with increments of 1 in each plot.

Returning to the discussion on the turbulent flame speed and brush thickness, we note the following interesting feature regarding the quantities $S_{T,0}/S_L$ and δ_T. Similar to the kinetic energy K and the dissipation rate ε in flow turbulence, the quantities δ_T and $S_{T,0}/S_L$ form the pairs as the zeroth and second moments of the energy spectrum and flame surface spectrum, respectively. Although a square root is involved in the turbulent flame speed expression, the similarity between $(\delta_T, S_{T,0}/S_L)$ and (K, ε), emerging from their definitions, is observed in their respective integrands, and hence in the spectra presented in Figs. 8(a) and 8(b).

Figures 8(a) and 8(b) show, respectively, the spectra of Γ and $k^2\Gamma$ versus k for various $U_{\rm rms}/S_L$. It is clear from Fig. 8(a) that for small $U_{\rm rms}/S_L$ no $-5/3$ power dependence is observed, and the spectrum is dominated by exponentially decaying dissipation effects. As expected, the $-5/3$ dependence emerges for higher $U_{\rm rms}/S_L$, and the spectra in Figs. 8(a) and 8(b) appear to saturate. This leads to a rapid saturation of the flame brush thickness and to the experimentally well-known nonlinear "bending" behavior of the turbulent flame speed. The bending is also clearly inherent in the nonlinear expression for the turbulent flame speed. The dominance of the higher wave numbers in the $k^2\Gamma$ spectrum in Fig. 8(b) also indicates that fine-scale turbulence controls the total flame surface area generated, and thus the necessity of very high spatial resolution for experimental or numerical determination of turbulent flame speed. Also for the same reason it could be conjectured that the large scatter in the turbulent flame speed data is inherent in the definition, for being second moment it requires an order of magnitude larger sample space than that would be required for convergence of statistic δ_T.

To superpose the effects of DL instability on $S_{T,0}$ derived in Eq. (56), i.e., on the turbulent flame speed without accounting for the effect of DL instability, which could be considered to be proportional to area A_T, we take a step back into the Damköhler derivation on the basis of mass conservation

$$S_{T,0}/S_L = A_T/A_0, \tag{58}$$

where A_T is the turbulent flame surface area without considering DL instability and A_0 is the projected area. Thus in the event of no DL instability, when the effect of turbulence is the only mechanism of flame surface corrugation, and $g = g(x_1, x_2)$, we find

$$\frac{S_{T,0}}{S_L} = \frac{1}{A_0}\int_{A_0}\int \sqrt{1+\nabla g\cdot\nabla g}\, dx_1 dx_2 = \frac{A_0\langle\sqrt{1+\nabla g\cdot\nabla g}\rangle}{A_0} = \langle\sqrt{1+\nabla g\cdot\nabla g}\rangle. \tag{59}$$

However, when DL instability competes with turbulence providing an additional corrugation mechanism, the projected area, over which the integral in Eq. (59) is taken, should be replaced by $A_{\rm DL,turb}$. Physically, this implies that turbulence is generating surface area over an already increased area produced by the instability. Considering $S_{\rm DL,turb}/S_L = A_{\rm DL,turb}/A_0$, with $S_{\rm DL,turb}$ given by Eq. (24), we obtain the expression for S_T accounting for DL instability. Consequently,

$$\frac{S_T}{S_L} = \frac{1}{A_0}\int\int_{A_{\rm DL,turb}} \sqrt{1+\nabla g\cdot\nabla g}\, dx_1 dx_2 = \frac{A_{\rm DL,turb}}{A_0}\langle\sqrt{1+\nabla g\cdot\nabla g}\rangle = \frac{S_{\rm DL,turb}}{S_L}\langle\sqrt{1+\nabla g\cdot\nabla g}\rangle, \tag{60}$$

where Eq. (24) should be substituted for $S_{\rm DL,turb}$, which thus emerges as a correction superposed on the expression for the turbulent flame speed obtained without considering DL instability. Figure 9 presents the plot of $S_{T,0}/S_L$ [Eq. (59)], and S_T/S_L [Eq. (60)], with $S_{\rm DL,turb}$ given by Eq. (24), which means that self-similarity is adopted for all $\lambda_I \geqslant \tilde{\lambda}_c$. These results were obtained by numerical integration of Eqs. (56) and (60), while the exact analytical forms for special cases will be presented in the next section. These scaled flame speeds versus $U_{\rm rms}/S_L$ for various $\lambda_I/\delta_L = 10^2, 10^3, 10^4$ are shown in Fig. 9. For small $U_{\rm rms}/S_L \leqslant 1$, the quantity $S_{T,0}/S_L$ shows a quadratic behavior inherent in its definition, Eq. (56), and is in accordance with the Clavin-Williams theory where a weakly perturbed periodic flow is considered [4]. In a different viewpoint by Kerstein and Ashurst [7] and Mayo and Kerstein [57], weak turbulence is considered white noise which

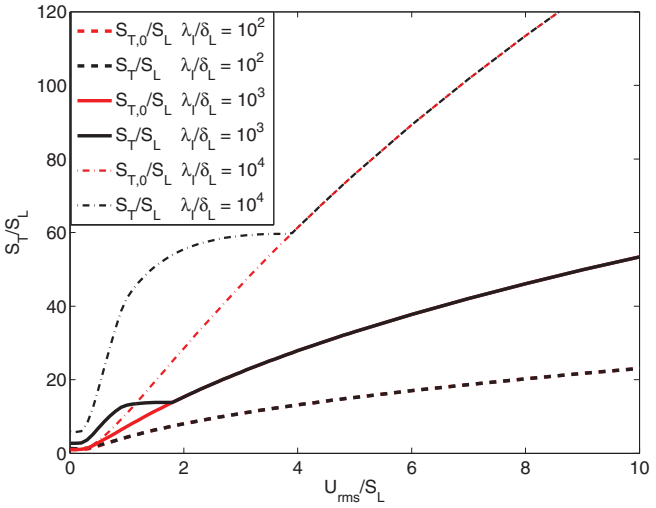

FIG. 9. (Color online) Scaled turbulent flame speed without and with DL instability, $S_{T,0}/S_L$ and S_T/S_L,respectively, versus the scaled turbulent intensity $U_{\rm rms}/S_L$ for various $\lambda_I/\delta_L = 10^2, 10^3$, and 10^4.

yields a $U_{\rm rms}^{4/3}$ dependence for the turbulent burning velocity. Since white noise is uncorrelated with a flat spectrum, which is far from the model adopted here even for weak turbulence, recovery of the Clavin-Williams result is reasonable in the present work. For higher $U_{\rm rms}/S_L$, the value $S_{T,0}/S_L$ increases almost linearly, to a final bend resembling a power law with a subunity exponent. With increasing λ_I at a given $U_{\rm rms}/S_L$, the quantity $S_{T,0}/S_L$ monotonically increases simply due to the increased scale separation, which increases the area under the $k^2\Gamma$ spectrum. Superimposing the correction for DL instability on $S_{T,0}$, we find S_T/S_L, which collapses on $S_{T,0}/S_L$ at large $U_{\rm rms}/S_L$, when corrugation by DL instability is destroyed by turbulence, and as expected from the modified regime diagram in Fig. 5. However, at small and moderate $U_{\rm rms}/S_L$ it is clearly seen that the hydrodynamic instability, in its domain of influence, can amplify the turbulent flame speed by more than a factor of 2, depending on the scale separation. The flat regions and cusps of the S_T/S_L curve occur due to the assumption that the instability vanishes sharply at the corresponding regime boundary, i.e., when $\lambda_I = \tilde{\lambda}_c$, while in reality such a transition could be much smoother.

D. Analytical form of turbulent flame speed for $c_1 = 0$

Here we derive the exact form of the turbulent flame speed $S_{T,0}/S_L$ for the particular case of $c_1 = 0$. As discussed in Sec. III C, the coefficient for the $k\Gamma$ term is expected to be small, as the kinematic restoration and gas expansion terms both scale as $k\Gamma$ in the Fourier space but with opposite signs, which was also shown by DNS [39]. Hence, the limit of $c_1 = 0$ is indeed a case of physical interest, and as it removes the first exponential term of Eq. (36), the integration of Eq. (55) can be performed analytically. Specifically, Eq. (36) with $c_1 = 0$ can be rewritten as

$$\Gamma(k) = Bk^{-5/3}\exp(-\Psi\tilde{k}^{4/3}) \tag{61}$$

for $\tilde{k} \geqslant 1$, and $\Gamma = 0$ otherwise, with $\tilde{k} \equiv k/k_I$ and

$$\Psi = \frac{3}{4}(2\pi)^{4/3} c_2 \left(\frac{U_{\rm rms}}{S_L}\right)^{-1}\left(\frac{k_I}{k_M}\right) = \frac{3}{4}(2\pi)^{4/3} c_2 \,{\rm Mk}\left(\frac{U_{\rm rms}}{S_L}\frac{\lambda_I}{\delta_L}\right)^{-1}. \tag{62}$$

We next evaluate the constant B in Eq. (61). This can be done only for large $U_{\rm rms}/S_L$, when the turbulent flame brush thickness is about the integral length scale, $\delta_T \sim \lambda_I$. It has been shown by DNS [55] that the ratio δ_T/λ_I quickly saturates to $\sim$1.4 at moderate $U_{\rm rms}/S_L$ and stays constant at large $U_{\rm rms}/S_L$, which is also evident from Fig. 8(a), demonstrating saturation of the area under the corresponding $\Gamma(k)$ curves for large $U_{\rm rms}/S_L$. It is noted that the error from approximating $\delta_T = \lambda_I$ (a prefactor of 1.4) and that from Eq. (41), i.e., averaging under the square root (a prefactor of 0.75), tend to cancel out each other, which allows the overall approximation constant to be near unity. To avoid ambiguity, hereafter we set $U_{\rm rms}/S_L$ to achieve its maximum possible value within the corrugated flamelets regime to evaluate B. At the boundary of this regime, ${\rm Ka}_{\delta_L} = 1$, we have

$$(U_{\rm rms}/S_L)_{\rm max} = (\lambda_I/\delta_L)^{1/3}. \tag{63}$$

With the result (63), Eq. (62) becomes

$$\Psi = \Psi^* = \tfrac{3}{4}(2\pi)^{4/3} c_2\,{\rm Mk}\,(\lambda_I/\delta_L)^{-4/3}. \tag{64}$$

With $(U_{\rm rms}/S_L)_{\rm max} \sim O(10)$ and $c_2 \sim {\rm Mk} \sim O(1)$, we evaluate Ψ^* from Eqs. (63) and (64) as $\Psi^* \sim O(10^{-3})$. Then the flame brush thickness is given by

$$\begin{aligned}\delta_T^2 &\equiv \int_{k_I}^{\infty}\Gamma(k)\,dk = Bk_I^{-2/3}\int_1^{\infty}\tilde{k}^{-5/3}\exp(-\Psi^*\tilde{k}^{4/3})\,d\tilde{k}\\ &= \frac{3}{2}Bk_I^{-2/3}\{\exp(-\Psi^*) - \sqrt{\pi\Psi^*}\,{\rm erfc}(\sqrt{\Psi^*})\}\\ &\approx \frac{3}{2}Bk_I^{-2/3}\exp(-\Psi^*) \approx \frac{3}{2}Bk_I^{-2/3}.\end{aligned} \tag{65}$$

Substituting Eq. (65) into Eq. (57), we find

$$B = \tfrac{2}{3}k_I^{2/3}\lambda_I^2 = \tfrac{8}{3}\pi^2 k_I^{-4/3}. \tag{66}$$

Consequently, the scalar spectrum function [Eq. (61)] becomes

$$\Gamma(k) = \tfrac{8}{3}\pi^2 k_I^{-3}\tilde{k}^{-5/3}\exp(-\Psi\tilde{k}^{4/3}), \tag{67}$$

and Eqs. (56) and (67) state the generalized formula for the scaled turbulent flame speed,

$$\begin{aligned}\frac{S_{T,0}}{S_L} &= \sqrt{1 + \int_{k_I}^{\infty}k^2\Gamma(k)\,dk}\\ &= \sqrt{1 + \frac{8\pi^2}{3}\int_1^{\infty}\tilde{k}^{1/3}\exp(-\Psi\tilde{k}^{4/3})\,d\tilde{k}}\\ &= \sqrt{1 + \frac{2\pi^2}{\Psi\,\exp\,\Psi}},\end{aligned} \tag{68}$$

with Ψ given by Eq. (62). In systems of practical relevance, $\lambda_I/\lambda_L \sim O(10) - O(10^3)$, $U_{\rm rms}/S_L \sim O(1) - O(10)$, and $c_2 \sim {\rm Mk} \sim O(1)$. Hence, Eq. (62) typically yields $\Psi \ll 1$, or

at least $\Psi < 1$. In the event of $\Psi \ll 1$, we have $\exp(\Psi) \sim 1$, and Eq. (68) is reduced to

$$\frac{S_{T,0}}{S_L} = \pi \left(\frac{2}{\Psi}\right)^{1/2} = \frac{2^{5/6}\pi^{1/3}}{(3c_2\,\mathrm{Mk})^{1/2}} \left(\frac{U_{\mathrm{rms}}}{S_L}\frac{\lambda_I}{\delta_L}\right)^{1/2} \sim \left(\frac{U_{\mathrm{rms}}}{S_L}\frac{\lambda_I}{\delta_L}\right)^{1/2}. \quad (69)$$

Retaining the exponential term, the exact analytical form is given by

$$\left(\frac{S_{T,0}}{S_L}\right)^2 = 1 + \left(\frac{2^{5/3}\pi^{2/3}}{3c_2\,\mathrm{Mk}}\right)\left(\frac{U_{\mathrm{rms}}}{S_L}\right)\left(\frac{\lambda_I}{\delta_L}\right) \times \exp\left[\frac{3}{4}(2\pi)^{4/3} c_2\,\mathrm{Mk}\left\{-\left(\frac{U_{\mathrm{rms}}}{S_L}\right)^{-1}\left(\frac{\lambda_I}{\delta_L}\right)^{-1}\right\}\right]. \quad (70)$$

The power law of Eq. (69) for the scaled turbulent flame speed is revealing as it can be scaled as $\sqrt{\mathrm{Re}_T}$ considering unity Schmidt number. The same scaling was obtained by Damköhler in the 1930s [1] but for thin reaction zones with the argument that when fine-scale turbulence penetrates the preheat zone, diffusivity of the laminar flame is replaced by the turbulent diffusivity, while the chemical time scale remains the same [1,12]. Simple algebra then yields the $\sqrt{\mathrm{Re}_T}$ dependence. In contrast, our analysis is valid in both the corrugated flamelet and thin reaction zone regimes. We nevertheless note that the associated global length scale for a turbulent flame is the turbulent flame brush thickness δ_T rather than the laminar flame thickness δ_L, since δ_T is the scale to be affected by the turbulent transport. In particular, any average scalar gradient spans over δ_T instead of δ_L, and hence δ_T has to be used to define the turbulent diffusivity. Consequently, to replace the diffusivity of a laminar flame with the turbulent diffusivity for a turbulent flame, it is only necessary that turbulent eddies penetrate the flame brush thickness, which is always the case. It is noted that the turbulent diffusivity is a purely convective flow property and is not related to molecular diffusion, hence its associated length or time scales should be the convective instead of diffusion scales. This scaling of $\sqrt{(U_{\mathrm{rms}}/S_L)(\lambda_I/\delta_L)}$ is also reported in some experimental correlations, summarized in detail in the review by Driscoll [2] and hence suggests the general validity of the analytical results obtained herein.

Another feature to be explored is the pressure dependence. Increasing pressure reduces the flame thickness, and hence new wave numbers become accessible for flame wrinkling. Thus the increased scale separation should amplify the scaled turbulent flame speed at higher pressures as has been observed experimentally [58,59]. To incorporate the pressure dependence we can write

$$\frac{\delta_{L,p}}{\delta_{L,p0}} = \left(\frac{p}{p_0}\right)^{-\alpha}, \quad (71)$$

where the subscripts p_0 and p denote the standard atmospheric and modified pressures, respectively. Based on the numerical simulations with detailed chemical kinetics [60], the exponent in Eq. (71) has been reported as $\alpha = 0.58$ for methane-air flames at $\varphi = 0.9$, $\mathrm{Le} = 1$. Consequently,

$$\frac{\lambda_I}{\delta_{L,p}} = \frac{\lambda_I}{\delta_{L,p0}}\frac{\delta_{L,p0}}{\delta_{L,p}} = \frac{\lambda_I}{\delta_{L,p0}}\left(\frac{p}{p_0}\right)^{\alpha}, \quad (72)$$

and Eq. (62) becomes

$$\Psi = \frac{3}{4}(2\pi)^{4/3} c_2\,\mathrm{Mk}\left(\frac{U_{\mathrm{rms}}}{S_L}\frac{\lambda_I}{\delta_{L,p0}}\right)^{-1}\left(\frac{p}{p_0}\right)^{-\alpha}, \quad (73)$$

with the counterpart of Eq. (69), $\Psi \ll 1$, being

$$\left(\frac{S_{T,0}}{S_L}\right)^2 = \frac{2^{5/3}\pi^{2/3}}{(3c_2\,\mathrm{Mk})}\left(\frac{U_{\mathrm{rms}}}{S_L}\frac{\lambda_I}{\delta_{L,p0}}\right)\left(\frac{p}{p_0}\right)^{\alpha}, \quad (74)$$

while the exact form, Eq. (70), becomes

$$\left(\frac{S_{T,0}}{S_L}\right)^2 = 1 + \left(\frac{2^{5/3}\pi^{2/3}}{3c_2\,\mathrm{Mk}}\right)\left(\frac{U_{\mathrm{rms}}}{S_L}\right)\left(\frac{\lambda_I}{\delta_{L,p0}}\right)\left(\frac{p}{p_0}\right)^{\alpha} \times \exp\left[\frac{3}{4}(2\pi)^{4/3} c_2\,\mathrm{Mk}\left\{-\left(\frac{U_{\mathrm{rms}}}{S_L}\right)^{-1}\left(\frac{\lambda_I}{\delta_{L,p0}}\right)^{-1} \times \left(\frac{p}{p_0}\right)^{-\alpha}\right\}\right]. \quad (75)$$

The results (74) and (75) are compared to the experimental data [58,59] in Figs. 10(a) and 10(b). Kobayashi and co-workers [58,59] have reported the combustion consumption speeds over a wide range of scaled turbulence intensities, pressures, and length scales in a Bunsen configuration for methane-air mixtures at the equivalence ratio $\phi = 0.9$, where $\mathrm{Le} = 1.0$ with respect to the inert and $\mathrm{Le} \approx 0.96$ with respect to mixture-averaged properties. Moreover, the authors of [59] measured the flame surface area at the progress variable $\langle c \rangle = 0.1$ contours, which typically resides within the inner core of the jet and hence is mostly uncontaminated by large-scale shear layer structures. Consequently, direct comparison to the present analysis is possible, as the derived turbulent flame speeds are essentially consumption speeds in nearly homogenous isotropic turbulence. It is further noted that all the experimental conditions fall outside the instability domain in Fig. 5, and hence $S_{T,0}/S_L$ should be sufficient to describe the reported data. Figure 10(a) then shows the comparison in a log-log plot with abscissas and ordinates in the same convention as that in [58,59] to highlight the slopes of the data sets at constant pressure ratios and the dependence on pressure. The constants used for evaluating the analytical expression for all the data sets are $c_2 = 1.5, \mathrm{Mk} = 2, \alpha = 0.58$, $\lambda_I = L_{\mathrm{geometric}}/2.5$, and $\delta_{L,p0} = 0.5$ mm. The ratio of the geometric to integral length scales is assumed to be 2.5 such that $\lambda_I/\delta_{L,p0}$ exactly corresponds to the values specified in [59]. It is seen that good quantitative agreement exists for the slopes and the shift due to pressure, despite the large scatter in the experimental data. Figure 10(b) is a counterpart of Fig. 10(a) in a linear plot, but with the abscissa being $\sqrt{(U_{\mathrm{rms}}/S_L)(\lambda_I/\delta_{L,p})}$, i.e., the right-hand side of Eq. (69) is used as an independent variable. Considering the large scatter, it is seen that the data largely collapse onto a straight line, hence indicating good agreement between the proposed theoretical expression and experimentation. It is interesting to note that in the experiments of [58] and according to a general belief,

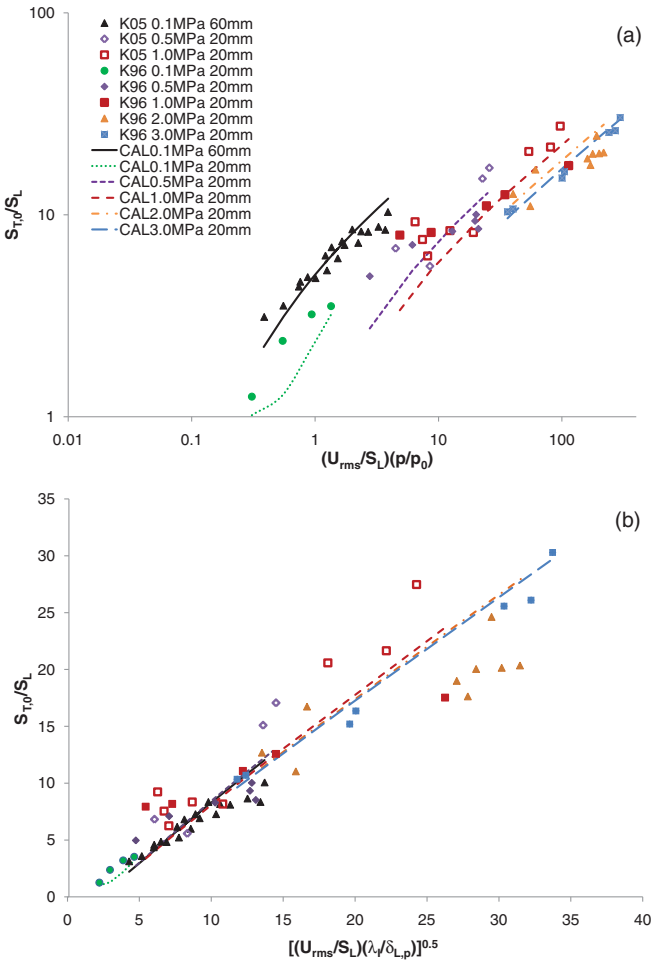

FIG. 10. (Color online) (a) Log-log plot of normalized turbulent flame speed versus normalized turbulent intensity times normalized pressure to compare analysis with experimental data from Kobayashi *et al*. [58,59]. Symbols: Experiment; Lines: Analytical expression with corresponding color: Eq. (70). (b) Plot of normalized turbulent flame speed versus right-hand side of Eq. (69) to collapse the experimental data on a straight line. Legends are the same in both (a) and (b).

the increase in the turbulent flame speed with pressure is attributed to DL instability. We note, however, that all the experimental conditions are outside the DL-affected regime according to the diagram in Fig. 5, and concurrently Eqs. (69) and (70) show the explicit dependence of the turbulent flame speed on the flame thickness, the decrease of which facilitates the increased turbulent flame speed very similar to that in the case of DL instability, where the cutoff is an explicit function of the flame thickness. Moreover, it can be readily shown that the dimensional turbulent flame speed $S_{T,0} \sim (U_{\rm rms})^{0.5}(p/p_0)^{0.08}$, i.e., $S_{T,0}$, has negligible dependence on pressure when $S_L \sim (p/p_0)^{-0.5}$ as assumed in [58]. This negligible dependence of $S_{T,0}$ on pressure is also consistent with the dimensional turbulent flame speed results presented in [58].

The discrepancy at small $U_{\rm rms}/S_L$ is inherent as the self-similar inertial range description of Kolmogorov's theory, and subsequently Pao's theory, is valid at moderate to large Reynolds numbers. However, even at moderate Reynolds numbers, when viscous dissipative effects cause a sharper falloff for the kinetic energy spectrum, the error introduced by osculating the corresponding flame spectrum is partly accounted for by flame dissipation mechanisms, and hence the leading-order contribution is captured. It is noted that both decays are exponential terms as in the flame spectrum of Eq. (36) or the model spectrum of Pope [33] for fluid turbulence. Finally, it is emphasized that all the results presented in this section are obtained with the approximation of Eq. (41). This approximation holds well for all moderate to large R_λ, which are practically encountered in turbulent premixed combustion. For extreme R_λ, the approximation error can also be accounted for following Kolmogorov's refined similarity hypothesis [53]. In that case the normalized turbulent flame speed should scale as $S_T/S_L \sim (U_{\rm rms}/S_L)^{0.5}(\lambda_I/\delta_L)^{0.5-\mu_g/4}$, i.e., a deviation from $(\lambda_I/\delta_L)^{0.5}$ scaling may be observed.

IV. SUMMARY

In this investigation we have estimated conditions in which DL instability could compete with turbulence to induce corrugation of a flame front. The limiting condition at which turbulence can completely suppress corrugation of the flame surface due to DL instability has been characterized by a dimensionless parameter β Eq. (14), shown to be the ratio of the instability and turbulence time scales at a given length scale, which exceeds unity. Such a boundary has been presented in the traditional turbulent combustion regime diagram for identification of zones where the instability effects should be considered while predicting global turbulent premixed combustion properties such as the turbulent flame speed. In this regard, the concept of a turbulence-induced DL cutoff was introduced, a function of which evolved as a correction on the turbulent flame speed without considering DL instability. The turbulent flame speed in the absence of DL instability was derived from the spectral closure of the G equation, thus considering the multiscale nature of turbulence-the central feature of turbulent flows. Superimposing the correction by DL instability consideration on the DL-stable turbulent flame speed, we present the final form of the normalized turbulent flame speed as a function of the normalized turbulence intensity. Finally, an analytical expression for the turbulent flame speed is obtained by realistically setting one of the dissipation mechanisms to be negligible. The analytical expression is found to agree closely with the experimental data from Kobayashi and co-workers [58,59] over a wide range of normalized turbulence intensity and pressure. At large normalized turbulence intensities, the normalized turbulent flame speed is found to scale as $\sqrt{(U_{\rm rms}/S_L)(\lambda_I/\delta_L)}$, which is an observed experimental correlation in other configurations as well.

ACKNOWLEDGMENTS

Participants of this research were supported by the Combustion Energy Frontier Research Center, an Energy Frontier Research Center funded by the US Department of Energy, Office of Basic Energy Sciences under Award No. DE-SC0001198, and by the US Air Force Office of Scientific Research. We sincerely acknowledge discussions with Professor Dipak

K. Dey of the University of Connecticut on the statistical approximations. We also thank Professor Hong G. Im of the University of Michigan, Dr. Alan R. Kerstein of Sandia National Laboratories, Professor Norbert Peters of RWTH Aachen University, and Professor Stephen B. Pope of Cornell University for their comments.

[1] N. Peters, *Turbulent Combustion* (Cambridge University Press, New York, 2000).
[2] J. F. Driscoll, Prog. Energy Combust. Sci. **34**, 91 (2008).
[3] A. N. Lipatnikov and J. Chomiak, Prog. Energy Combust. Sci. **36**, 1 (2010).
[4] P. Clavin and F. A. Williams, J. Fluid Mech. **90**, 589 (1979).
[5] V. Yakhot, Combust. Sci. Technol. **60**, 191 (1988).
[6] A. R. Kerstein, W. T. Ashurst, and F. A. Williams, Phys. Rev. A **37**, 2728 (1988).
[7] A. R. Kerstein and W. T. Ashurst, Phys. Rev. Lett. **68**, 934 (1992).
[8] A. Pocheau, Phys. Rev. E **49**, 1109 (1994).
[9] B. Denet, Phys. Rev. E **55**, 6911 (1997).
[10] F. A. Williams, *Combustion Theory* (Benjamin Cummings, Menlo Park, CA, 1985).
[11] Ya. B. Zeldovich, G. I. Barenblatt, V. B. Librovich, and G. M. Makhviladze, *Mathematical Theory of Combustion and Explosion* (Consultants Bureau, New York, 1985).
[12] C. K. Law, *Combustion Physics* (Cambridge University Press, New York, 2006).
[13] G. Searby and P. Clavin, Combust. Sci. Technol. **46**, 167 (1986).
[14] H. Boughanem and A. Trouve, Proc. Combust. Inst. **27**, 971 (1998).
[15] V. Bychkov, Phys. Rev. E **68**, 066304 (2003).
[16] V. Akkerman and V. Bychkov, Combust. Theory Modell **9**, 323 (2005).
[17] V. Bychkov, A. Petchenko, and V. Akkerman, Combust. Sci. Technol. **179**, 137 (2007).
[18] V. Akkerman, V. Bychkov, and L.-E. Eriksson, Combust. Flame **151**, 452 (2007).
[19] N. Peters, J. Fluid Mech. **242**, 611 (1992).
[20] P. Pelce and P. Clavin, J. Fluid Mech. **124**, 219 (1982).
[21] M. Matalon and B. J. Matkowsky, J. Fluid Mech. **124**, 239 (1982).
[22] P. Clavin and P. Garcia, J. Mec. **2**, 245 (1983).
[23] V. Bychkov and M. Liberman, Phys. Rep. **325**, 115 (2000).
[24] G. Sivashinsky, Astronaut. Acta **4**, 1177 (1977).
[25] M. Frankel, Phys. Fluids A **2**, 1879 (1990).
[26] V. Bychkov, Phys. Fluids **10**, 2091 (1998).
[27] V. V. Bychkov, S. M. Golberg, M. A. Liberman, and L.-E. Eriksson, Phys. Rev. E **54**, 3713 (1996).
[28] V. Bychkov, S. Golberg, M. Liberman, A. Kleev, and L.-E. Eriksson, Combust. Sci. Technol. **129**, 217 (1997).
[29] O. Yu. Travnikov, V. V. Bychkov, and M. A. Liberman, Phys. Rev. E **61**, 468 (2000).
[30] Y. Gostintsev, A. Istratov, and Y. Shulenin, Combust., Explos. Shock Waves **24**, 563 (1988).
[31] D. Bradley, C. G. W. Sheppard, R. Woolley, D. A. Greenhalgh, and R. D. Lockett, Combust. Flame **122**, 195 (2000).
[32] G. Jomaas and C. K. Law, Proceedings of the 47th AIAA Aerospace Sciences Meeting and Exhibit, paper 1185 (2009).
[33] S. B. Pope, *Turbulent Flows* (Cambridge University Press, New York, 2000).
[34] F. Creta, N. Fogla, and M. Matalon, Combust. Theory Modell. **15**, 267 (2011).
[35] N. Peters, J. Fluid Mech. **384**, 107 (1999).
[36] A. N. Lipatnikov and J. Chomiak, Prog. Energy Combust. Sci. **28**, 1 (2002).
[37] N. Swaminathan and K. N. C. Bray, Combust. Flame **143**, 549 (2005).
[38] H. Kolla, N. Rogerson, and N. Swaminathan, Combust. Sci. Technol. **182**, 284 (2010).
[39] N. Peters, H. Wenzel, and F. A. Williams, Proc. Combust. Inst. **28**, 235 (2000).
[40] A. Dandekar and L. Collins, Combust. Flame **101**, 428 (1995).
[41] L. Collins and M. Ultisky, Proc. Combust. Inst. **26**, 315 (1996).
[42] T. Tran, P. Chakraborty, N. Guttenberg, A. Prescott, H. Kellay, W. Goldburg, N. Goldenfeld, and G. Gioia, Nat. Phys. **6**, 438 (2010).
[43] L. R. Collins, Comput. Fluids **24**, 663 (1995).
[44] M. Wirth and N. Peters, Proc. Combust. Inst. **24**, 493 (1992).
[45] Y. H. Pao, Phys. Fluids **8**, 1063 (1965).
[46] I. G. Shepherd, R. K. Cheng, T. Plessing, C. Kortschik, and N. Peters, Proc. Combust. Inst. **29**, 1833 (2002).
[47] S. Corrsin and O. M. Phillips, J. Soc. Indust. Appl. Math. **9**, 395 (1961).
[48] A. Soika, F. Dinkelacker, and A. Leipertz, Proc. Combust. Inst. **27**, 785 (1998).
[49] S. H. Kim and H. Pitsch, Phys. Fluids **19**, 115104 (2007).
[50] U. Frisch, *Turbulence* (Cambridge University Press, New York, 2000).
[51] R. B. Leipnik, J. Aust. Math. Soc., Ser. B: Appl. Math. **32**, 327 (1991).
[52] K. R. Sreenivasan and R. A. Antonia, Annu. Rev. Fluid Mech. **29**, 435 (1997).
[53] A. N. Kolmogorov, J. Fluid Mech. **13**, 82 (1961).
[54] C. H. Gibson, Proc. Roy. Soc. Lond. A **434**, 149 (1991).
[55] H. Wenzel and N. Peters, Combust. Sci. Technol. **177**, 1095 (2005).
[56] Y. Shim, S. Tanaka, M. Tanahashi, and T. Miyauchi, Proc. Combust. Inst. **33**, 1455 (2010).
[57] J. R. Mayo and A. R. Kerstein, Phys. Lett. A **372**, 5 (2007).
[58] H. Kobayashi, T. Tamura, K. Maruta, and T. Niioka, Proc. Combust. Inst. **26**, 389 (1996).
[59] H. Kobayashi, K. Seyama, H. Hagiwara, and Y. Ogami, Proc. Combust. Inst. **30**, 827 (2005).
[60] R. J. Kee, F. M. Rupley, and J. M. Miller: Chemkin II: A Fortran chemical kinetics package for analysis of gas-phase chemical kinetics, Report Number: SAND 89-8009, 2000.